Visible-light simultaneous photocatalysis of methyl orange and Cr(VI) in water by rare earth modified titanium dioxide

Yajun Wang*, Lijuan Jiang, Changgen Feng

State Key Laboratory of Explosion Science and Technology, Beijing Institute of Technology, Beijing 100081, China
Fax: +86 10 68912941; email: yajunwang@bit.edu.cn

ABSTRACT

A series of TiO_2 doped with rare earth elements La and Nd were synthesized via sol–gel technique. The as-prepared catalysts were characterized by powder X-ray diffraction (XRD), nitrogen adsorption-desorption analysis and scanning electron microscopy (SEM). Analytical results demonstrate that doping of La and Nd could inhibit the agglomeration of TiO_2 particles, increase the surface area and decrease the crystallite size of TiO_2 with mesoporous structures. By using the materials, visible-light ($\lambda \geq 420$ nm) photocatalysis activities for the reduction of hexavalent chromium Cr(VI) and degradation of methyl orange MO in composite system were investigated. The results show that the catalysts order by the photocatalytic efficiency in Cr(VI)-MO composite system is 1% $La/TiO_2 > 1\%$ $Nd/TiO_2 > TiO_2$. Methyl orange and Cr(VI) were totally eliminated by 1% La/TiO_2 in 30 min under the conditions: visible-light ($\lambda \geq 420$ nm), a 50 ml mixture of 40 mg/l MO and 20 mg/l Cr(VI), catalyst of 0.08 g dose and pH 1.0. Kinetic studies indicate that the reduction of Cr(VI) and degradation of MO in composite system were not in agreement with first-order kinetics very well due to synergistic effect in the simultaneous photocatalytic process.

Keywords: Titanium dioxide; Rare earth; Photocatalysis; Methyl orange; Cr(VI); Synergistic effect

1. Introduction

Semiconductor photocatalysis is a kind of catalytic reaction depending on light (usually UV), which was developed in 1972 [1] and thereafter developed to treat contaminant [2–4]. So far, TiO_2 is the most promising photocatalyst since its high activity, chemical stability, robustness against photocorrosion, low toxicity, and availability with low cost. And the photocatalysis reaction kinetics is generally described by Langmuir–Hinshelwood adsorption kinetic model [5] which is simplified as:

$$\ln C_0/C = kKt = K_{app}t \qquad (1)$$

where C_0 is the initial concentration of pollutant; C is the concentration of pollutant at time t; k is photocatalytic reaction rate constant; K is Langmuir adsorption constant; K_{app} is apparent first-order kinetics rate constant.

Though TiO_2 shows many advantages, there are two bottlenecks in application: one is the quick combination of photo-generated electrons and holes, and the other is the little sun utilization rate. Many researchers have tried to modify TiO_2 in order to reduce the combination of electrons and holes and increase the absorption scope of sunlight, such as rare earth (La, Ce, Pr, and Nd) modification [6–10], nonmetallic (F [11])

---

*Corresponding author.

modification, and composite catalyst [12–14]. Rare earth elements modification could suppress the transition of TiO_2 from anatase to rutile phase and make the catalyst particle size smaller and specific surface area larger than those of the nonmodified, and using rare earth elements to modify TiO_2 has been the popular method to improve the photocatalytic activity [15–17].

Photocatalysis could be used to deal with many pollutants, such as dye, pesticide, heavy metal ion, etc. Owing to that actual wastewater is almost mixture, much attention have been paid to the photocatalysis research in composite system. Furthermore, according to photocatalysis principle, photocatalytic oxidation and reduction reactions occurring simultaneously could reduce the combination of electrons and holes so as to improve catalytic efficiency. Composite pollutant system photocatalysis has been studied recently [18–20], but little compared with single ones. Prairie [21] first proposed the synergetic effect between the photocatalytic reduction and oxidation. The results show that the acids (organics) with high molecular weight show quicker reduction rates than the ones with small molecular weight; organics that can be oxidized directly by capturing hole show quicker reduction rates than the ones which are oxidized indirectly by ·OH.

The present research is focused on visible-light simultaneous photocatalysis of methyl orange (MO) and Cr(VI) in water by La- or Nd-modified TiO_2. Modified catalysts were characterized by various means. The competition of photocatalytic removal of MO and Cr(VI), under visible-light irradiation ($\lambda \geq 420$ nm) was employed to investigate the photocatalytic activity of the catalysts.

2. Experimental

2.1. Materials

All chemicals were purchased from Sinopharm Chemical Reagent Co., China and employed without any further purification. Lanthanum nitrate hexahydrate ($La(NO_3)_3 \cdot 6H_2O$), neodymium nitrate hexahydrate ($Nd(NO_3)_3 \cdot 6H_2O$), absolute ethyl alcohol (EtOH), acetone (C_3H_6O), diphenylcarbazide ($C_{13}H_{13}N_4O$), potassium dichromate ($K_2Cr_2O_7$), hydrochloric acid (HCl), perchloric acid ($HClO_4$), phosphoric acid (H_3PO_4), sulfuric acid (H_2SO_4), and methyl orange (MO) are analytical grade reagents. Tetrabutyl titanate ($Ti(OBu)_4$) is chemical grade. The water for experiments is deionized water.

2.2. Catalysts preparation

TiO_2 was synthesized via sol–gel process, following the specific procedures. A mixture of $Ti(OBu)_4$ (10 ml) and EtOH (30 ml) was stirred under room temperature. HCl was added into the mixture to obtain pH 1.5, and the solution was marked A. The mixed solution containing H_2O (2 ml), and EtOH (4 ml) was marked B. Then, B was added dropwise into A during 10 min approximately. The resulting acidic mixture was stirred constantly until sol was obtained; subsequently, the sol was maintained for 24 h until gel formation. The gel was dried at 333 K until no decrease in its weight and then calcinated at 823 K for 3 h with a heating rate of 5 K/min. The preparation method of La-TiO_2 or Nd-TiO_2 was similar to TiO_2 except that lanthanum nitrate hexahydrate (La$(NO_3)_3 \cdot 6H_2O$) or neodymium nitrate hexahydrate (Nd$(NO_3)_3 \cdot 6H_2O$), as the rare earth precursor, was dissolved into H_2O (2 ml). The rare earth doping amount was calculated by La or Nd element.

2.3. Characterization

The crystalline phases of the prepared catalysts were characterized by powder X-ray diffraction (XRD) on a PANalytical X′ Pert PRO MPD diffractometer using Cu Kα radiation that was operated at 40 kV and 40 mA. The specific surface area and pore structure were determined from adsorption-desorption isotherms of nitrogen by a Quantachrome NOVA 2200e instrument using multipoint BET and BJH methods. Surface morphologies were observed by scanning electron microscope (SEM) (Hitachi S-4800 N) operating at 15.0 kV.

2.4. Photocatalytic procedures

The photocatalytic experiments were performed on an open photoreactor. The light source is provided by a PLS-SXE300UV Xe lamp (300 W) with emission of $\lambda \geq 420$ nm (using a 420 nm cut-off filter), which is positioned above the photoreactor. The initial concentration (C_0) of MO and Cr(VI) was fixed at 40 mg/l and 20 mg/l, respectively, both in single system and in composite system, with pH ca. 1 adjusted by $HClO_4$. The prepared catalyst (80 mg) was suspended into a fresh MO/Cr(VI) single solution (50 ml) or MO-Cr(VI) mixed solution (50 ml). At given interval of illumination, a sample of suspension (ca. 1 ml) was taken out and filtered with microporous membrane (0.45 μm). The absorbance of residual MO in solution was analyzed by an APL 752 UV–vis spectrometer at 510 nm. Then, the degradation rates of MO d_{MO} were calculated. The absorbance of residual Cr(VI) in solution was determined by diphenylcarbazide colorimetric method at 540 nm [22], with $d_{Cr(VI)}$ the reduction rate. When the concentration was greater than the

detection limit, the operation of dilution was necessary. For MO-Cr(VI) composite system, two absorbances were determined according to MO and Cr(VI) concentration test methods, respectively, and then, the concentrations were calculated by solving equations with double wavelength method.

3. Results and discussion

3.1. Characterization of the catalysts

3.1.1. XRD analysis

Fig. 1 shows the XRD results of the catalysts. It can be observed that the XRD patterns of Nd-doped TiO$_2$, La-doped TiO$_2$, and pure TiO$_2$ are similar, and all crystallized in the anatase phase with characteristic diffraction peaks ($2\theta = 25.3°$ (101), 37.1° (004), 48.1° (200), 53.9° (105), 62.7° (211)) [9]. Intensity of each absorption peak is different among the samples, and absorption peaks of TiO$_2$ are sharper than those of the doped TiO$_2$. Nd and La modification made the crystallinity of TiO$_2$ weak. No characteristic peaks of La and Nd are found due to that the doping amount is small, and La$_2$O$_3$ and Nd$_2$O$_3$ are highly dispersed [23].

3.1.2. Nitrogen adsorption-desorption analysis

Table 1 gives the results of nitrogen adsorption-desorption analysis for the samples which indicates the mesoporous nature of all catalyst materials. The BET surface area of 1% Nd-TiO$_2$ and 1% La-TiO$_2$ are 80.8 m^{2}g^{-1} and 80.6 m^{2}g^{-1}, respectively, two times more than that of TiO$_2$. The high surface area confirms that the doped samples have better thermal stability than pure TiO$_2$ and the formed rare earth titania
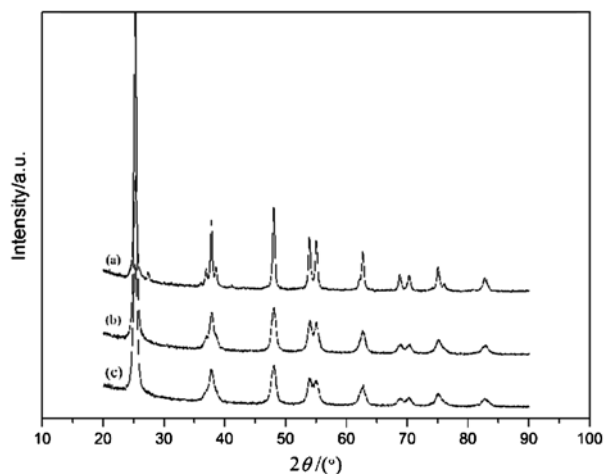
Fig. 1. XRD patterns of prepared samples: (a) TiO$_2$; (b) Nd-TiO$_2$; (c) La-TiO$_2$.

Table 1
Microstructure of the prepared catalysts

Materials	S_{BET} (m^{2}g^{-1})	Average pore radius (nm)	Pore volume (cm^{3}g^{-1})
TiO$_2$	40.2	6.4	0.98
1% La-TiO$_2$	80.6	6.3	0.98
1% Nd-TiO$_2$	80.8	4.9	0.98

composite oxides effectively enhance the surface area and decrease the crystallite size of TiO$_2$ [10]. The addition of Nd or La did not change the pore volume of TiO$_2$, and the addition of La almost did not change the average pore radius of TiO$_2$, while Nd make pore radius reduce significantly. Different pore structures of La-TiO$_2$ and Nd-TiO$_2$ make the photocatalytic activities different.

3.1.3. SEM observation

The SEM micrographs of the materials (Fig. 2) reveal that particle sizes of Nd-TiO$_2$ and La-TiO$_2$ are much smaller than that of TiO$_2$. The particles of all catalysts are found to be in spherical shape. Unlike Nd-TiO$_2$ and La-TiO$_2$, pure TiO$_2$ particles are found to be in the form of aggregation. Nd and La modification preferably retard the aggregation and improve the growth of well-dispersed particles. The slight difference between La-TiO$_2$ and Nd-TiO$_2$ lies in that La and Nd have different electronic structures and radius. Ionic radius of La^{3+} (0.102 nm) and Nd^{3+} (0.0995 nm) are bigger than that of Ti^{4+} (0.068 nm), and therefore, it is difficult for La^{3+} or Nd^{3+} to really enter into the lattice of TiO$_2$. Ti–O–La or Ti–O–Nd bond could be formed at the interface, and La^{3+} and Nd^{3+} exist in the particle wall of the obtained samples [10,24].

3.2. Photocatalytic activity

All experiments were repeated by three times. Control tests found that no detectable concentration decrease occurred in single MO and Cr(VI) solution or MO-Cr(VI) composite solution under visible-light irradiation ($\lambda \geq 420$ nm), at pH ca. 1 without catalysts [25], and less than 5% MO concentration decreased in MO single system under the action of catalysts in visible-light irradiation. Therefore, MO and Cr(VI) have no apparent chemical reaction at short time with pH ca. 1, and the degradation of MO in MO single system did not happen with catalysts under visible-light irradiation.
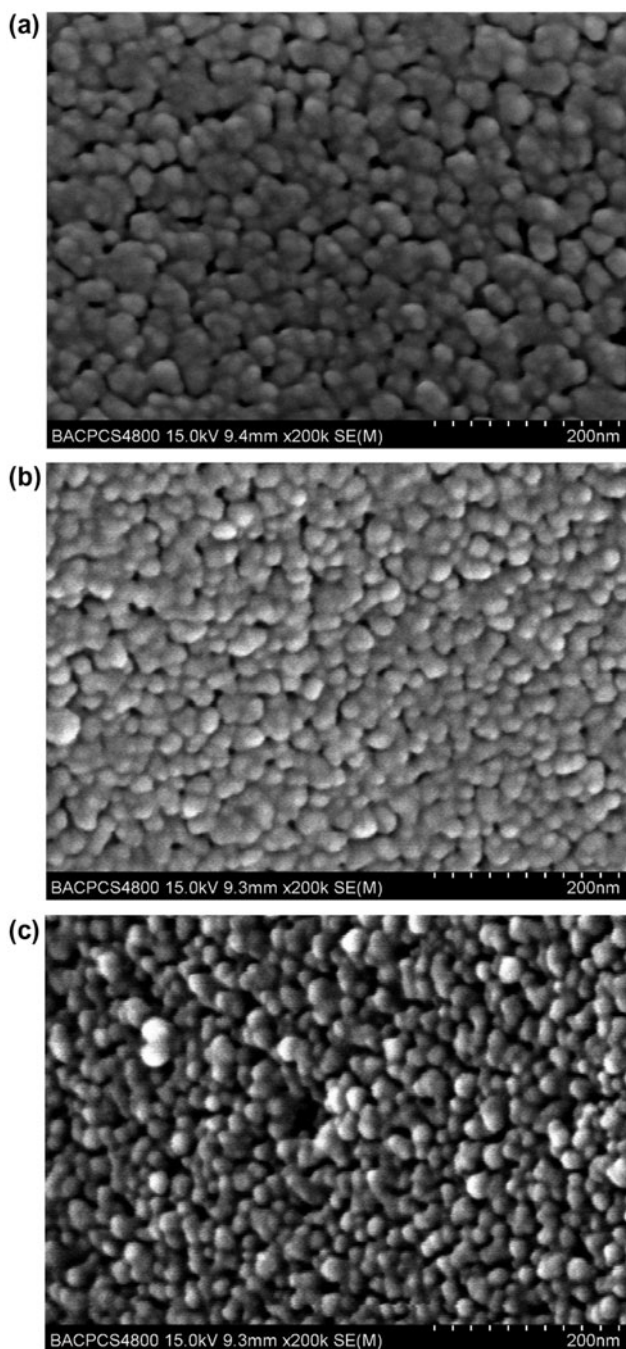
Fig. 2. SEM images of prepared samples.

3.2.1. Photocatalytic reduction of Cr(VI)

Catalysts used in the test were 80 mg, and pH of Cr(VI) solution was adjusted by $HClO_4$ to ca. 1. Figs. 3 and 4 give the results of photocatalytic reduction of Cr(VI) in the presence of Nd-TiO_2 and La-TiO_2. The results show that Nd and La modification improve the photocatalytic activity of reduction and different doping amount of Nd-TiO_2 and La-TiO_2 present slightly different catalytic efficiency. From the characterization above, the surface area of La-TiO_2 and Nd-TiO_2 are two times more than that of TiO_2, and photocatalytic removal of Cr(VI) in solution by both TiO_2 and modified TiO_2 are mainly caused by adsorption. Little visible-light photocatalytic activity for Cr(VI) may be due to charge imbalance would occur owing to the formation of Ti–O–La, which might affect the photocatalytic activity of catalyst [24]. When ions doping amount is high, the space charge region becomes very narrow and the penetration depth of light into TiO_2 greatly exceeds the space charge layer, so electron-hole pairs will recombine easily [26]. Consequently, there is an optimum concentration of dopant ions. From Figs. 3 and 4, less than 50% reduction rate of Cr(VI) was achieved in 100 min by TiO_2 with 1% doping amount of Nd and La.

3.2.2. Simultaneous photocatalysis of Cr(VI) and MO

Simultaneous photocatalysis of Cr(VI) and MO were performed in 50 ml composite solution, with 20 mg/l Cr(VI)-40 mg/l MO, results shown in Figs. 5–8. Single MO could not be removed by TiO_2 under visible-light irradiation, and single Cr(VI) was removed very slowly by TiO_2 under visible-light irradiation according to Figs. 3 and 4, while they can be removed easily in the composite system. MO was completely decolored and Cr(VI) was almost completely reduced in 40 min. Simultaneous photocatalysis of Cr(VI) and MO can improve the photocatalytic efficiency of TiO_2, which is mainly due to the synergistic effect. Recombination of electrons and holes was suppressed in Cr(VI)-MO composite system, and
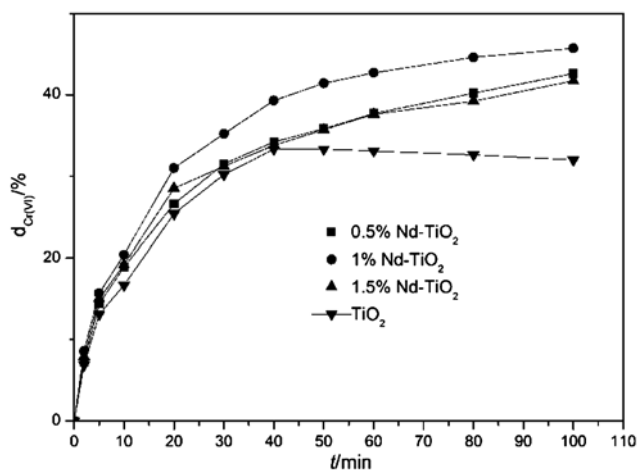
Fig. 3. Photocatalytic reduction of Cr(VI) in Cr(VI) solution by Nd-TiO_2.
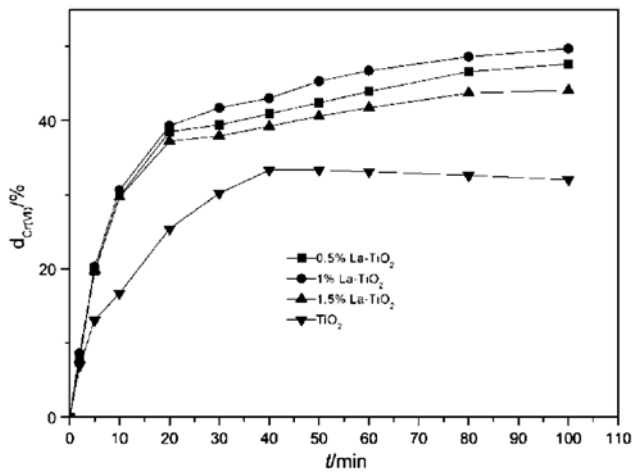
Fig. 4. Photocatalytic reduction of Cr(VI) in Cr(VI) solution by La-TiO$_2$.
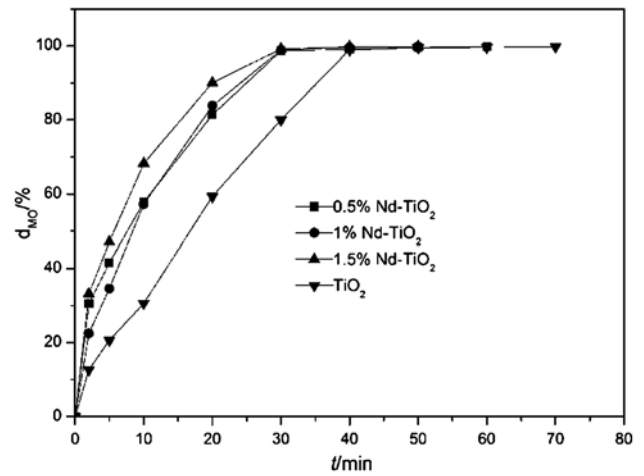
Fig. 6. Photocatalytic degradation of MO in Cr(VI)-MO system by Nd-TiO$_2$.
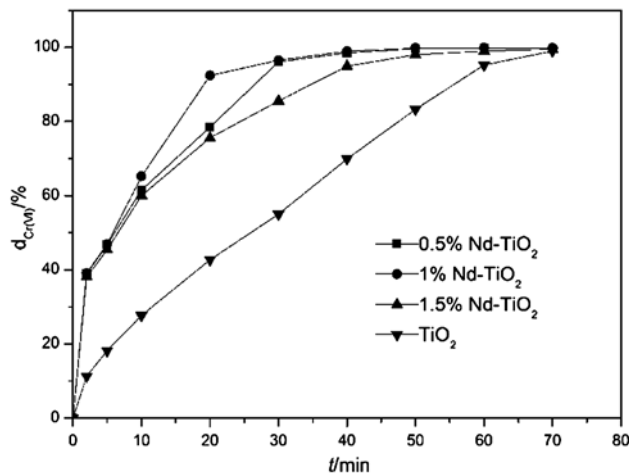
Fig. 5. Photocatalytic reduction of Cr(VI) in Cr(VI)-MO system by Nd-TiO$_2$.
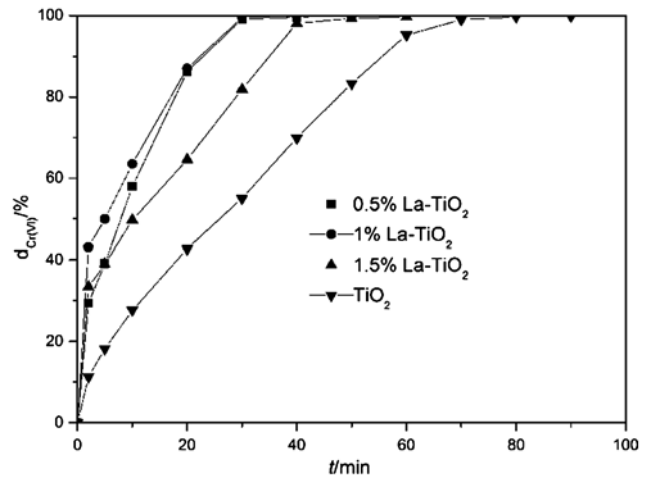
Fig. 7. Photocatalytic reduction of Cr(VI) in Cr(VI)-MO system bby La-TiO$_2$.

electrons and holes were fully utilized. The photo-reduction of Cr(VI) to Cr(III) and oxidation of organics can be achieved via a photocatalytic process with a simplified mechanism as follows [27].

$$TiO_2 + hv \rightarrow e^- + h^+ \quad (2)$$

$$Cr(VI) + H^+ + e^- \rightarrow Cr(III) + H_2O \quad (3)$$

$$H_2O + h^+ \rightarrow O_2 + H^+ \quad (4)$$

$$H_2O + h^+ \rightarrow \cdot OH + H^+ \quad (5)$$

$$\cdot OH + organics \rightarrow \cdots \rightarrow CO_2 + H_2O \quad (6)$$

$$h^+ + organics \rightarrow \cdots \rightarrow CO_2 + H_2O \quad (7)$$
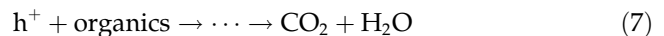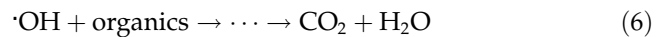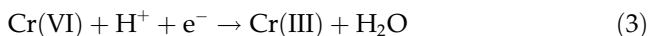
Sometimes, the intermediates of MO photocatalytic degradation could reduce Cr(VI) to Cr(III), which can be achieved, for example, via a photocatalytic process with a simplified mechanism as follows [28] in methyl alcohol–Cr(VI) composite system.

$$CH_3OH + h^+ \rightarrow CH_3^\cdot \quad (8)$$

$$Cr(VI) + CH_3^\cdot \rightarrow Cr(III) + products \quad (9)$$
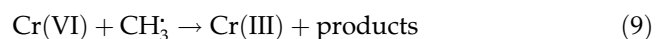
1% Nd-TiO$_2$ and 1% La-TiO$_2$ have larger specific surface area than that of TiO$_2$, and they could adsorb more Cr(VI) or MO and electrons and holes are more easier to reach the catalyst surface to react. La and Nd are Lewis acid, which can form Lewis acid–base complexes with MO [10]. La and Nd doping also change the surface structure of TiO$_2$. As a result, 1% Nd-TiO$_2$ and 1% La-TiO$_2$ can remove Cr(VI) and MO in 30 min in the composite photocatalysis system. Especially, the reduction of Cr(VI) in composite system was accelerated significantly compared with the one in single system. There are many factors affecting the simultaneous photocatalysis, such as catalyst (surface area, crystalline phase, electronic structure and surface properties, etc.), the mass ratio of MO/Cr(VI), pH, intermediate products of reaction. Composite system photocatalysis needs to be designed effectively to

achieve good synergistic effect for catalytic oxidation and reduction [21].

3.2.3. Kinetics analysis

The composite aqueous solution, 50 ml with 20 mg/l Cr(VI)–40 mg/l MO, was selected to investigate the kinetics of removal of Cr(VI) and degradation of MO under visible-light irradiation, and the results were shown in Figs. 9 and 10 and Tables 2 and 3. Figs. 9 and 10 show that 1% La/TiO$_2$ has the biggest rate of Cr(VI) removal and degradation of dye, then
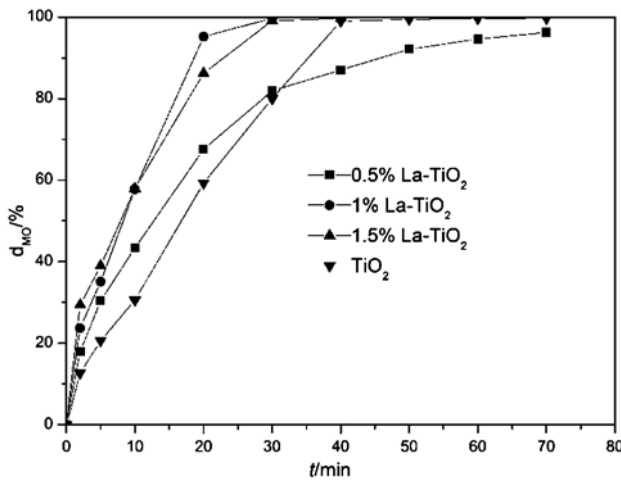
Fig. 8. Photocatalytic degradation of MO in Cr(VI)-MO system by La-TiO$_2$.
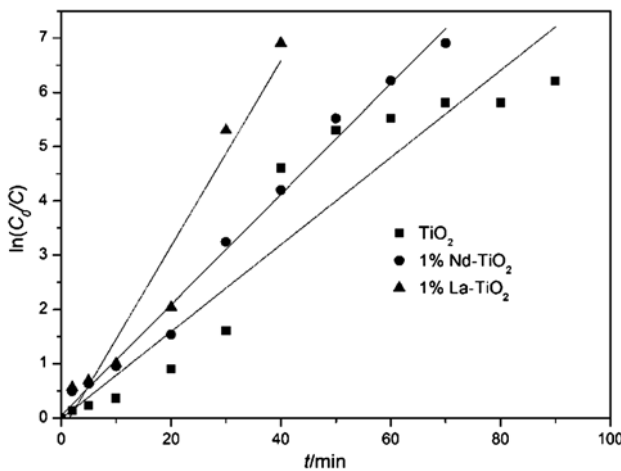
Fig. 9. Photocatalytic degradation kinetics for MO.
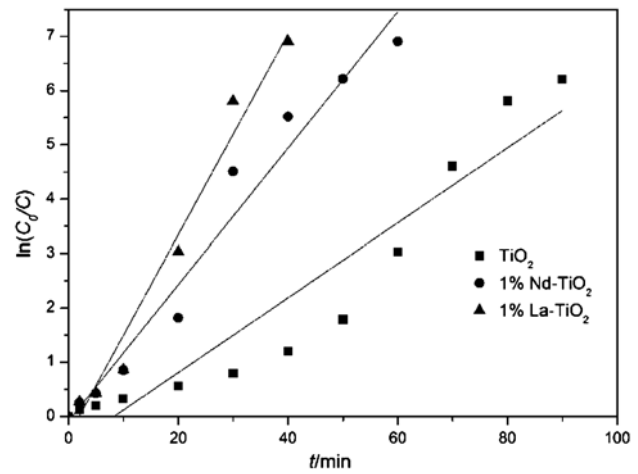
Fig. 10. Photocatalytic reduction kinetics for Cr(VI).

Table 2
Apparent first-order kinetics equations and relative parameters for photocatalytic degradation of MO with different catalysts in composite system

Materials	Kinetics equations	K_{app} (min^{-1})	$t_{1/2}$ (min)	R^2
TiO$_2$	$\ln(C_0/C) = 0.080t + 0.013$	0.080	8.6	0.904
Nd-TiO$_2$	$\ln(C_0/C) = 0.101t - 0.048$	0.101	6.8	0.988
La-TiO$_2$	$\ln(C_0/C) = 0.171t - 0.2559$	0.171	4.1	0.943

Table 3
Apparent first-order kinetics equations and relative parameters for photocatalytic removal of Cr(VI) with different catalysts in composite system

Materials	Kinetics equations	K_{app} (min^{-1})	$t_{1/2}$ (min)	R^2
TiO$_2$	$\ln(C_0/C) = 0.068t - 0.570$	0.068	10.2	0.904
Nd-TiO$_2$	$\ln(C_0/C) = 0.125t - 0.048$	0.125	5.5	0.967
La-TiO$_2$	$\ln(C_0/C) = 0.185t - 0.355$	0.185	3.7	0.973

1% Nd-TiO$_2$. Tables 2 and 3 show that the reduction rate of Cr(VI) and degradation rate of MO in the composite system were not in agreement with first-order kinetics very well (the biggest value of R^2 is 0.988). And the kinetics of 1% La/TiO$_2$ and 1% Nd/TiO$_2$ catalysis are more likely to be the apparent first-order kinetics than that of TiO$_2$ photocatalysis. In six curves of Figs. 9 and 10, there is a sudden jump, where photocatalytic synergistic effect is the most significant and photocatalytic rate is the fastest. The earlier this jump happens, the earlier photocatalytic synergistic effect appears.

4. Conclusions

La and Nd modification can make effective improvement of photocatalytic activity both in single system and in composite system, which is mainly due to the increase in surface area and decrease in the particle size of TiO$_2$. Cr(VI) or MO single system could not be photocatalyzed or photocatalytic effect is not obvious in visible-light irradiation, while in the composite system, effective visible-light photocatalysis happens easily. Since the existence of catalytic synergism, removal rate of Cr(VI) and MO are improved substantially. Although Nd and La are both lanthanoid elements, but different atomic radius and extranuclear electron arrangement make the microstructure of the doped TiO$_2$ different, which results in slightly different photocatalytic activities. The reduction rate of Cr(VI) and degradation rate of MO in composite system were not in agreement with first-order kinetics very well.

References

[1] A. Fujishima, K. Honda, Electrochemical photolysis of water at a semiconductor electrode, Nature 238 (1972) 37–38.
[2] D. Robert, A. Piscopo, J.V. Weber, First approach of the selective treatment of water by heterogeneous photocatalysis, Environ. Chem. Lett. 2 (2004) 5–8.
[3] W.R. Shen, W.K. Zhao, F. He, Y.L. Fang, TiO$_2$ photocatalytic reactions and its applications in wastewater treatment, Prog. Chem. 10 (1998) 349–361.
[4] M.D. Ward, J.M. White, A.J. Bard, Electrochemical investigation of the energetics of particulate titanium dioxide photocatalysis-the methyl viologen-acetate system, J. Am. Chem. Soc. 105 (1983) 27–31.
[5] I.K. Konstantinou, T.A. Albanis, TiO$_2$-assisted photocatalytic degradation of azo dyes in aqueous solution: Kinetic and mechanistic investigations: A review, Appl. Catal. B 49 (2004) 1–14.
[6] X.Q. Ou, J.P. Meng, Q.M. Wang, J.M. Yu, Enhanced photoactivity of layered nanocomposite materials containing rare earths, titanium dioxide and clay, J. Rare Earths 24 (2006) 251–254.
[7] C.M. Fan, P. Xue, Y.P. Sun, Preparation of nano-TiO$_2$ doped with cerium and its photocatalytic activity, J. Rare Earths 24 (2006) 309–313.
[8] D. de la Cruz Romero, G. Torres Torres, J.C. Are´valo, R Gomez, A. Aguilar-Elguezabal, Synthesis and characterization of TiO$_2$ doping with rare earths by sol–gel method: Photocatalytic activity for phenol degradation, J. Sol-Gel Sci. Technol. 56 (2010) 219–226.
[9] J.J. Xu, Y.H. Ao, D.G. Fu, C.W. Yuan, Study on photocatalytic performance and degradation kinetics of X-3B with lanthanide-modified titanium dioxide under solar and UV illumination, J. Hazard. Mater. 164 (2009) 762–768.
[10] K.M. Parida, S. Nruparaj, Visible light induced photocatalytic activity of rare earth titania nanocomposites, J. Mol. Catal. A 287 (2008) 151–158.
[11] J.J. Jiang, M.C. Long, D.Y. Wu, W.M. Cai, Preparation of F-modified nanosized TiO$_2$ and its methyl orange photodegradation mechanism, Chin. J. Phys. Chem. 27 (2011) 1149–1156.
[12] S.B. Rawal, S.D. Sung, W.I. Lee, Novel Ag$_3$PO$_4$/TiO$_2$ composites for efficient decomposition of gaseous 2-propanol under visible-light irradiation, Catal. Commun. 17 (2012) 131–135.
[13] Y. Yang, Y.H. Guo, C.W. Hu, C.J. Jiang, E.B. Wang, Synergistic effect of Keggin-type $[X^{n+}W_{11}O_{39}]^{(12-n)-}$ and TiO$_2$ in macroporous hybrid materials $[X^{n+}W_{11}O_{39}]^{(12-n)-}$-TiO$_2$ for the photocatalytic degradation of textile dyes, J. Mat. Chem. 13 (2003) 1686–1694.
[14] Y.J. Wang, K.C. Lu, C.G. Feng, Photocatalytic degradation of methyl orange by polyoxometalates supported on yttrium-doped TiO$_2$, J. Rare Earths 29 (2011) 866–871.
[15] J.H. Li, X. Yang, X.D. Yu, L.L. Xu, W.L. Kang, W.H. Yan, H.F. Gao, Z.H. Liu, Y.H. Guo, Rare earth oxide-doped titania nanocomposites with enhanced photocatalytic activity towards the degradation of partially hydrolysis polyacrylamide, Appl. Surf. Sci. 255 (2009) 3731–3738.
[16] W.Y. Zhou, S.Q. Tang, S.Y. Zhang, X. Zhou, L. Wan, Preparation and photocatalytic properties of nano- TiO$_2$ photocatalysts doped with various rare earth, J. Chin. Ceram. Soc. 32 (2004) 1203–1208.
[17] W.Q. Lu, D.Q. Wang, X.Q. He, L.M. Zhao, Catalytic degradation of Rhodamine B in TiO$_2$ doped with gadolinium or two rare earth elements in visible light, J. Rare Earths 25 (2007) 427–431.
[18] X.H. Feng, S.M. Ding, F. Wu, N.S. Deng, B. Nikolai, Simultaneous photoreduction of Cr(VI) and photooxidation of methyl orange in water induced by Fe(III)-OH complex, Res. Environ. Sci. 18 (2005) 75–78.
[19] X.F. Lei, X.X. Xue, Visible light-induced photocatalytic reduction of Cr(VI) in presence of methyl orange and titania-bearing blast furnace slag photocatalysts, J. Northeast. Univer. (Nat. Sci.) 32 (2011) 1133–1136.
[20] T. Papadam, N.P. Xekoukoulotakis, I. Poulios, D. Mantzavinos, Photocatalytic transformation of acid orange 20 and Cr (VI) in aqueous TiO$_2$ suspensions, J. Photochem. Photobiol. A 186 (2007) 308–315.
[21] M.R. Prairie, L.R. Evans, B.M. Stange, S.L. Martinez, An investigation of titanium dioxide photocatalysis for the treatment of water contaminated with metals and organic chemicals, Environ. Sci. Technol. 27 (1993) 1776–1782.
[22] Editorial Committee of Water and Wastewater Monitoring Method, State Environmental Protection Administration, Water and Wastewater Monitoring Method, fourth ed., China Environmental Science Press, Beijing, 2002.
[23] Z.L. Shi, F.M. Liu, S.H. Yao, Preparation and photocatalytic activity of B, Y co-doped nanosized TiO$_2$ catalyst, J. Rare Earths 28 (2010) 737–741.

[24] F.B. Li, X.Z. Li, M.F. Hou, Photocatalytic degradation of 2-mercaptobenzothiazole in aqueous La^{3+}-TiO_2 suspension for odor control, Appl. Catal. B 48 (2004) 185–194.

[25] L.J. Jiang, Y.J. Wang, C.G. Feng, Simultaneous photocatalysis of methyl orange and Cr(VI) in water by TiO_2, J. Saf. Environ. 12 (2012) 109–113.

[26] A.W. Xu, Y. Gao, H.Q. Liu, The preparation, characterization, and their photocatalytic activities of rare-earth-doped TiO_2 nanoparticles, J. Catal. 207 (2002) 151–157.

[27] L.M. Wang, N. Wang, L.H. Zhu, H.W. Yu, H.Q. Tang, Photocatalytic reduction of Cr(VI) over different TiO_2 photocatalysts and the effects of dissolved organic species, J. Hazard. Mater. 152 (2008) 93–99.

[28] S. Chakrabarti, B. Chaudhuri, S. Bhattacharjee, A.K. Ray, B.K. Dutta, Photo-reduction of hexavalent chromium in aqueous solution in the presence of zinc oxide as semiconductor catalyst, Chem. Eng. J. 153 (2009) 86–93.